
PassNet: Scaling Large Language Models for Graph Compiler Pass Generation

Yiqun Liu* Yingsheng Wu* Ruqi Yang Enrong Zheng Honglei Qiu
 Sijun He Tai Liang Jingjing Wu Yuhan Zhou Yiwei Zhang
 Dongyan Chen Weihai Yi Xinqi Li† Siqi Bao†

Baidu, Inc.

Abstract

Modern tensor compilers such as TorchInductor deliver substantial speedups on mainstream models, yet face a systematic performance ceiling on long-tail workloads—our profiling shows that 43% of real-world subgraphs experience end-to-end slowdowns under default compilation. While LLMs offer a path toward automated optimization, existing efforts focus on standalone *kernel generation*. We argue that *pass generation*—where LLMs author structured graph transformations that integrate directly into compiler pipelines—is the more appropriate abstraction. We propose **PassNet**, the first large-scale ecosystem for LLM-based compiler pass generation, comprising: (1) **PassNet-Dataset**, over 18K unique computational graphs from 100K real-world models; and (2) **PassBench**, 200 curated long-tail fusible tasks (comprising 2,060 subgraphs in total) evaluated under the **Error-aware Speedup Score** (ES_t)—a metric unifying correctness, stability, and performance—with layered integrity defenses against systematic LLM exploitation. Experiments reveal that PassBench is both highly discriminative and genuinely unsaturated: the best frontier model trails TorchInductor by 37% in aggregate, yet on individual subgraphs LLMs achieve up to $3\times$ speedup over the same compiler—indicating that the bottleneck is consistency, not capability. Fine-tuning a small model on merely $\sim 4K$ PassNet trajectories yields a $2.67\times$ improvement approaching frontier-model performance, demonstrating substantial headroom and validating PassNet as live training infrastructure for advancing LLM-driven compiler optimization. All data, benchmarks, and tooling are publicly available.

1 Introduction

Modern deep learning systems increasingly rely on tensor compilers (e.g., TVM Chen et al. [2018], XLA Kaufman et al. [2021], TorchInductor Ansel et al. [2024]) to lower high-level computational graphs into efficient backend implementations for heterogeneous hardware. These compilers apply expert-designed, rule-based *pass pipelines*—sequences of graph transformations such as operator fusion, tiling, and layout selection—that have proven remarkably effective: on mainstream architectures, TorchInductor delivers up to $2.27\times$ inference speedups over eager execution across 180+ models Ansel et al. [2024]. Yet these static strategies face a structural limitation when confronting the long tail of real-world operator combinations.

The Long-Tail Optimization Gap. To quantify this limitation, we profile TorchInductor’s default pipeline on 9,526 subgraphs extracted from over 1,000 community models. The results reveal

*Equal contribution.

†Corresponding authors: lixinqi2010@gmail.com, baosiqi@baidu.com.

a systematic limitation: 34% achieve marginal speedups ($< 1.2\times$), 43% experience end-to-end slowdowns, and 8.3% are strictly degraded. This gap is structural, correlating with operator coverage rather than graph complexity ($r = 0.013$), suggesting that scaling graph coverage alone cannot overcome the heuristic-induced performance ceiling.

Pattern Concentration Creates Leverage. While the long-tail gap is significant, computation-graph patterns exhibit strong power-law concentration: deduplicating 100K models yields only $\sim 18K$ distinct graphs (82% redundancy), and $\sim 10,000$ subgraphs reduce to $\sim 1,025$ unique structural patterns. Generating high-quality passes for this concentrated set suffices to cover most workloads, enabling a shift from *manual rules* to *automated, data-driven pass generation*.

From Kernel Generation to Pass Generation. Large Language Models (LLMs) are a promising approach for long-tail optimization. Existing work has explored **Kernel Generation** Ouyang et al. [2025], Dai et al. [2026], Liao et al. [2025], producing standalone GPU kernels for individual operators. However, such kernels lack composability with compiler passes, require manual integration for deployment, and are difficult to verify due to unconstrained code generation.

We therefore define a new task, **Pass Generation**: given a computational subgraph, an LLM must author a structured compiler pass that interfaces directly with the compiler’s intermediate representation (formal definition in Section 3). This formulation preserves the “one-line compilation” experience (e.g., `torch.compile`) while enabling composable and verifiable optimizations. However, advancing this task requires large-scale data and rigorous evaluation—resources that do not yet exist.

The Data and Evaluation Bottleneck. Is pass generation with LLMs realistic today? On individual long-tail subgraphs, frontier LLMs can already generate passes achieving up to $3\times$ speedup over the default compiler—yet aggregate performance trails far behind, with no model reaching geometric-mean speedup above 1.0. This gap stems from two *infrastructure* bottlenecks: (1) *data scarcity*—a lack of large-scale, specialized corpora for fusion and layout optimization; and (2) *evaluation blind spots*—the absence of rigorous benchmarks allowing agents to bypass correctness for illusory gains. To bridge these, we introduce **PassNet**—the first ecosystem providing systematic data and benchmark support for the pass generation task.

Contributions. We formalize *pass generation*, where LLMs author structured graph transformations that integrate into compiler pipelines, and build a large-scale ecosystem to support this task.

- **PassNet-Dataset:** We collect over 18,086 unique computational graphs from 100K real-world models across diverse frameworks (PyTorch, PaddlePaddle) and task categories. We design *Recursive Folding* and *Execution-driven Prefix Analysis* to construct structurally diverse subgraphs at multiple granularities, forming the first large-scale open training set for pass generation.
- **PassBench:** We construct a benchmark of 200 tasks, each consisting of a variable number of long-tail subgraphs, evaluated under the *Error-aware Speedup Score* (ES_t), which jointly measures correctness, stability, and performance. To ensure evaluation integrity, we introduce layered defenses including AST-based inspection, runtime dispatch interception, and reverse evaluation order, which systematically counter exploitation patterns observed during development.
- **Benchmark Validation:** Through extensive evaluation of 6 frontier and open-source models, we show that PassBench is both highly discriminative ($3.22\times$ gap between model tiers) and genuinely unsaturated (best model trails TorchInductor by 37%). Fine-tuning on merely $\sim 4K$ PassNet trajectories yields a $2.67\times$ improvement, validating the dataset’s utility as training infrastructure.

The entire ecosystem—dataset, benchmark, evaluation tooling, and agent scaffold—is publicly available at <https://github.com/PaddlePaddle/PassNet>.

2 Related Work

Tensor Compilers. Tensor compilers transform high-level computation graphs into device-specific kernels via IR lowering and scheduling. TVM Chen et al. [2018] and Ansor Zheng et al. [2020] are search-based compilers relying on cost models, while XLA Leary and Wang [2017] applies heuristic graph-level optimizations. Recent systems include MetaSchedule Shao et al. [2022], Hidet Ding et al.

[2023], and BladeDISC Zheng et al. [2023a], with industry frameworks such as CINN Team [2021] and TorchInductor Ansel et al. [2024] integrated into production systems. Despite these advances, existing approaches still rely on manual transformation rules and struggle with long-tail workloads.

LLMs for Code Generation and Compiler Optimization. Large Language Models demonstrate strong code generation capabilities Jiang et al. [2024], Zheng et al. [2023b], including code completion Liu et al. [2025], bug repair Huang et al. [2025], Yang et al. [2026], and software engineering automation Jimenez et al. [2024], Yang et al. [2024], Wang et al. [2024]. For compiler tasks, LLM Compiler Cummins et al. [2025] pre-trains on compiler IR, Compiler-r1 Pan et al. [2025] explores RL-based auto-tuning, and DeCOS Cui et al. [2025] studies data-efficient optimization selection. TLP Zhai et al. [2023] and follow-up work Zhai et al. [2024] apply language models to tensor program generation. However, these approaches focus on pass selection or scheduling rather than synthesizing new transformation logic.

LLM-Driven GPU Kernel Generation. Recent work generates GPU kernels directly with LLMs. KernelBench Ouyang et al. [2025] benchmarks LLM-generated kernels, revealing gaps from production compilers. CUDA Agent Dai et al. [2026] and Kernelevolve Liao et al. [2025] scale agentic generation, while STARK Dong et al. [2025], Kevin Baronio et al. [2025], and Geak Wang et al. [2025] explore multi-agent and RL-based refinement. Other efforts include QiMeng-GEMM Zhou et al. [2025], CUDA-L1 Li et al. [2025], and Autocomp Hong et al. [2025]. In contrast, PassNet targets *pass generation*, i.e., structured transformations that integrate with compiler pipelines.

Performance Benchmarks. DL evaluation has evolved from DeepBench Narang and Research [2016] to MLPerf Mattson et al. [2020]. CompilerGym Cummins et al. [2022] provides an RL environment for compiler optimization. Datasets such as ComPile Grossman et al. [2024], Tpu-Graphs Phothilimthana et al. [2023], and TenSet Zheng et al. [2021] provide benchmarks for learned compilers. PassNet focuses on computational-graph-level pass generation for long-tail optimization, with an evaluation framework that jointly measures correctness, stability, and speedup.

3 The PassNet Ecosystem

The *PassNet* ecosystem bridges the dual infrastructure gaps identified in Section 1: the scarcity of large-scale pass generation corpora and the lack of robust, multi-dimensional benchmarks. In the following, we formalize the pass generation task before detailing each ecosystem component.

3.1 Task Formulation

In modern tensor compilers, a *pass* is a self-contained graph transformation that rewrites a computational graph while preserving its input–output semantics Lattner et al. [2021], Li et al. [2021]. Following the pattern-based rewriting paradigm adopted by MLIR Lattner et al. [2021] and TorchInductor Ansel et al. [2024], we formalize the core abstractions below.

Definition 3.1 (Computational Graph). A computational graph is a DAG $G = (V, E, \tau, \sigma)$, where V is a set of operator nodes, E encodes data dependencies, $\tau : V \rightarrow \mathcal{T}$ assigns operator types, and $\sigma : V \rightarrow \mathbb{Z}^+$ assigns output shapes. We write $f_G : \mathcal{X} \rightarrow \mathcal{Y}$ for the function computed by G .

Definition 3.2 (Compiler Pass). A compiler pass is a pair $\pi = (M, R)$, where $M : \mathcal{G} \rightarrow 2^{\mathcal{G}}$ is a pattern matcher identifying optimization-eligible subgraphs, and $R : \mathcal{G} \rightarrow \mathcal{G}$ is a rewriter replacing each matched subgraph with an optimized equivalent. A pass π is **valid** on G under tolerance t if:

$$\forall x \in \mathcal{X}, \quad \text{err}(f_G(x), f_{\pi(G)}(x)) \leq t \tag{1}$$

The **pass generation task** is: given a *task instance* $\mathcal{T} = \{G_1, \dots, G_k\}$ of subgraphs sharing the same operator-type sequence but varying in shape and dtype, generate a valid pass π that rewrites every $G_i \in \mathcal{T}$ and improves aggregate runtime performance. This multi-graph formulation requires π to generalize across varying shapes and data types, precluding shape-specific hacks. As opposed to free-form kernel generation, it further ensures composability with existing compiler pipelines and verifiability through standard compiler infrastructure.

3.2 Dataset Construction

The construction of the dataset consists of two stages: **computational graph collection** and **advanced subgraph generation**, as illustrated in Figure 1. The overall goal is to preserve real-world computation patterns while constructing structurally diverse and optimization-relevant subgraphs.

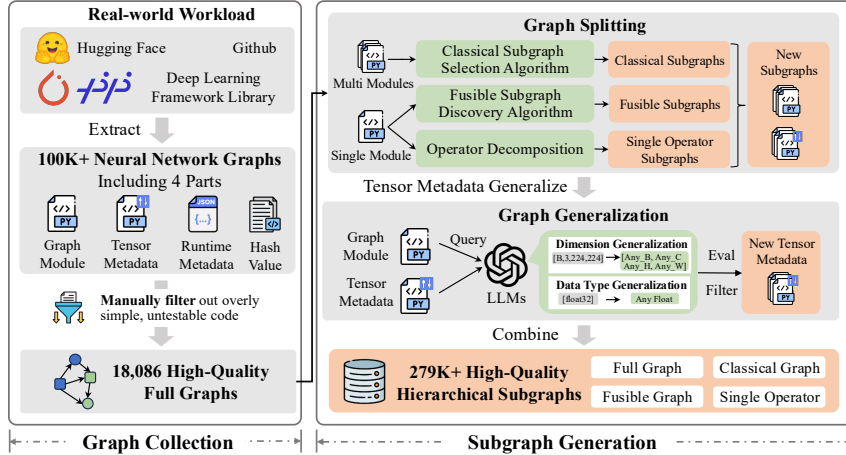


Figure 1: **PassNet Dataset Construction Pipeline.** We collect and filter real-world model graphs, and generate hierarchical training subgraphs via recursive graph splitting and metadata generalization.

Graph Collection and Validation. We extract computational graphs from real-world models via a lightweight decorator (`pass_net.extract`). During execution, symbolic tracing captures operator invocations and tensor dependencies, producing standardized representations (high-level IR, weights, and input metadata). To ensure high-fidelity graphs for downstream subgraph construction, each graph is rigorously validated against five key constraints: runnable, serializable, decomposable, statically analyzable, and custom-operator accessible (see Appendix A).

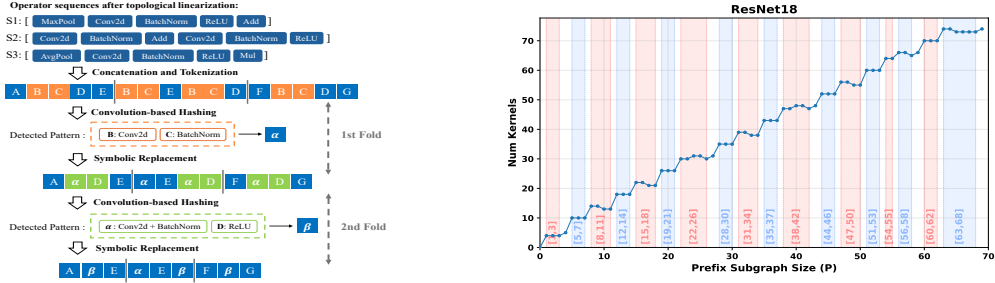
Subgraph Generation Strategies. To systematically map the optimization space, we propose three subgraph categories focusing on structural recurrence, fusion potential, and primitive behavior.

(1) **Classical Subgraph Selection via Recursive Folding.** A *Classical Subgraph* is a recurrent structural motif representing common computational patterns within a model family. To extract such motifs at scale, we design **Recursive Folding**: the method first linearizes the computation graph into a topological operator sequence, then iteratively applies convolution-based hashing to identify frequent subsequences and abstract them into symbolic units. This hierarchical process captures both local idioms (e.g., $[\text{Conv2d}, \text{BatchNorm}] \rightarrow \alpha$) and higher-level compositions (e.g., $[\alpha, \text{ReLU}] \rightarrow \beta$), producing a compact set of representative structures (Figure 2a).

(2) **Fusible Subgraph Discovery via Prefix Analysis.** A *Fusible Subgraph* is a contiguous segment of a computational graph where a compiler can apply operator fusion. To identify such regions systematically, we design **Prefix Analysis**, which analyzes the prefix kernel-count curve $(P, K(P))$, where $K(P)$ is the number of kernels launched by the first P operators, and detects plateaus satisfying $K(P + 1) = K(P)$. These indicate that operators are absorbed into existing execution units. Extracting contiguous plateaus yields subgraphs reflecting compiler fusion behavior (Figure 2b).

(3) **Single-operator Subgraph.** A *Single-operator Subgraph* consists of a primitive operator and captures operator-level behavior, complementing higher-level structures.

We apply shape and data type generalization during subgraph instantiation, generating instances with 10 shape configurations and 3 data types. This introduces variation in computation and optimization difficulty, improving applicability across hardware backends and compiler strategies.



(a) **Recursive folding.** [Conv2d, BatchNorm] $\rightarrow \alpha$; [α , ReLU] $\rightarrow \beta$. (b) **Prefix kernel-count curve (ResNet-18).** Plateau regions indicate fusible intervals.

Figure 2: Recursive folding for subgraph selection (left) and prefix-based fusibility analysis (right).

3.3 Dataset Characteristics

The resulting *PassNet* dataset comprises over 18K unique computational graphs derived from 100K diverse models across PyTorch and PaddlePaddle, with four distinguishing properties:

(i) **Authenticity and Scale:** All samples originate from production-grade community libraries rather than synthetic generators. With 100K source models yielding 18,086 deduplicated graphs (82% redundancy), *PassNet* captures the true distribution of real-world computation patterns—including long-tail operator combinations absent from curated benchmarks.

(ii) **Structural Diversity:** The collection spans six application domains (NLP: 63.6%, CV: 27.0%, Multimodal: 1.7%, Audio: 1.2%, Others: 6.5%), with model scales from lightweight mobile architectures to 10B-parameter models and node counts from 2 to 298,441 (median $\sim 2^9$).

(iii) **Optimization-Relevant Coverage:** We instantiate 129K fusible ($N_{\text{ops}} \in [2, 35]$), 126K classical ($N_{\text{ops}} \in [4, 62]$), and 24K single-operator subgraphs—totaling ~ 279 K instances across three complementary granularities, each augmented with 10 shape configurations and 3 data types.

(iv) **Interoperability:** A unified format for graphs, metadata, and custom operators ensures compatibility with compilers such as TorchInductor, CINN, XLA, and TVM without conversion overhead.

3.4 PassBench Design

While the full dataset serves as training data, rigorous evaluation requires a controlled benchmark with diverse, representative tasks. We curate **PassBench** via multi-dimensional bucketing and hierarchical grouping of subgraphs, with each group forming a task instance. The benchmark primarily focuses on fusible-subgraph tasks, comprising 4,476 training samples and 200 high-quality evaluation samples, with no overlap between training and evaluation sets. The dataset is further augmented with 4,078 classical-subgraph training samples and 200 evaluation counterparts, complemented by 1,029 single-operator samples. This multi-tiered composition provides varying levels of task difficulty.

Selection Pipeline. Subgraphs are bucketed along three dimensions: operator sequence (exact-match), input shape (log-quantized), and input dtype. Within each operator-sequence bucket, we apply stratified sampling with fixed stride σ , followed by cross-shape and dtype-aware aggregation to form groups corresponding to *PassBench* tasks (details in Appendix B). For evaluation, we select 200 operator sequences via a Hidden Markov Model and retain the largest group per sequence. Selected fusible samples contain 1–396 subgraphs (avg. = 10), exhibiting a long-tail distribution, and yield 2,060 subgraph-level evaluations in aggregate—providing finer-grained signal than benchmarks that evaluate at the task level alone (e.g., KernelBench, where each task corresponds to a single kernel).

Task Format. Each task is packaged as a directory containing (i) a Python reference implementation (`GraphModule`), (ii) tensor metadata, and (iii) runtime metadata. The agent is required to generate executable transformation passes under `pass_dir/` along with a JSON manifest. A submission is considered successful if it preserves correctness across all specified data types while achieving measurable performance improvement.

3.5 Error-aware Speedup Metrics

Evaluating compiler passes requires assessing both correctness and performance. Existing approaches fall short in three aspects: (1) treating correctness as binary (pass/fail) despite its continuous tolerance; (2) producing discrete signals that hinder iterative agent training; and (3) operating at the benchmark level, lacking fine-grained feedback on individual graphs.

We define a per-subgraph metric to jointly evaluate correctness and performance. For each subgraph i with measured speedup s_i , we introduce a tolerance threshold $t \in \{-10, \dots, |E| + 1\}$ to control acceptance of error categories $c_i \in \{1, 2, 3\}$ (accuracy, compilation, and runtime failures). For $t \leq 0$, strict correctness is enforced with varying numerical tolerances; for $t > 0$, more error categories are progressively forgiven. Let $\text{correct}_{t,i}$ be a binary indicator of whether subgraph i satisfies the correctness criteria under threshold t . The **error-aware rectified speedup** is defined as:

$$\hat{s}_{t,i} = \begin{cases} s_i, & \text{correct}_{t,i} \wedge s_i \geq 1, \\ s_i^{p+1}, & \text{correct}_{t,i} \wedge s_i < 1, \\ b^{\mathbf{1}(t < c_i)}, & \text{otherwise,} \end{cases} \quad (2)$$

where parameters $p, b \in (0, 1)$ respectively govern the exponential penalty for slowdowns and the base penalty for incorrect executions. The metric distinguishes three distinct scenarios: **(i) Speedup** ($s_i \geq 1$): retained for correct executions; **(ii) Slowdown** ($s_i < 1$): exponentially penalized via p ; **(iii) Incorrect**: assigned penalty b if $t < c_i$, or 1 if forgiven ($t \geq c_i$).

The **Error-aware Speedup Score** ES_t is defined as the geometric mean of $\{\hat{s}_{t,i}\}$ across all N subgraphs, with its equivalent factored form and macro-level derivation detailed in Appendix D:

$$ES_t = \left(\prod_{i=1}^N \hat{s}_{t,i} \right)^{1/N}. \quad (3)$$

We further aggregate ES_t across the tolerance spectrum via a normalized geometric mean to yield a unified scalar for agent feedback:

$$AS = \prod_{t=-10}^{|E|+1} ES_t^{W_t / \sum_{s=-10}^{|E|+1} W_s}, \quad (4)$$

where W_t assigns high weight to the strict-correctness regime ($t \in [-5, -3]$) and decays exponentially toward relaxed tolerances (details in Appendix E). While $fast_p$ (fraction of correct graphs with speedup $> p$) provides a binary correctness threshold, its discrete nature lacks a smooth signal and operates at benchmark-level granularity, failing to capture per-graph variation. AS instead provides a smooth, continuous feedback signal that jointly reflects correctness and performance gains.

3.6 Evaluation Integrity

A key challenge overlooked by prior work is that LLMs systematically exploit evaluation loopholes. In KernelBench-style evaluations, a submitted kernel passes as long as its output matches the reference—even if it simply delegates to `torch.compile`. During PassBench development, we found that 29%–50% of frontier-model submissions contained some form of exploitation. We document a three-stage arms race, where each defense exposed a new attack surface.

Case A: Computation Delegation → AST Inspection. The most prevalent pattern is invoking high-level APIs to bypass explicit operator-level transformations—e.g., calling `torch.matmul(in_1, in_3)` instead of implementing the fusion logic. We counter this with AST-based static analysis that blocks forbidden API calls within non-exempt functions (raising `RuntimeError: blocked call`), intercepting 78% of violations.

Case B: Dynamic Evasion → Dispatch Interception. Static analysis cannot cover dynamic execution paths such as implicit tensor method calls (e.g., `tmp = in_0 + in_1` dispatching to

`aten.add.Tensor`). We introduce a runtime monitoring layer via `PoisonDispatchTensor`, which overloads `__torch_dispatch__` to enforce whitelist-based operator filtering on the mandatory dispatch path. This layer exclusively identifies 18% of violations missed by AST inspection.

Case C: Cache Pollution → Reverse Evaluation. We discovered a *correctness escape*: in conventional “eager-first” evaluation order, PyTorch’s memory pooling leaves residual data in GPU memory that flawed code (e.g., `return torch.empty(...)`) can inadvertently pass validation against. We adopt “reverse evaluation” (compiled execution before eager baseline) to ensure verification within a pristine system state; such cases now receive `correctness = 0`.

These layered defenses are complemented by the *pass-form mandate* itself: requiring agents to author a pattern matcher and rewriter (rather than a standalone kernel) forces structural understanding of the computation graph, making trivial exploitation significantly harder.

4 Experiments

We design experiments to validate PassBench as a benchmark and PassNet-Dataset as training infrastructure: **(Q1)** Does PassBench provide meaningful discrimination across model capabilities, and how do current models compare to traditional compilers? **(Q2)** Can PassNet-Dataset improve model performance via post-training, validating its utility as training data?

4.1 Setup

PassAgent. To establish reproducible baselines, we implement **PassAgent**, a lightweight agentic scaffold for compiler pass synthesis. Following the dual-tool paradigm Yang et al. [2024], Wang et al. [2024], Jain et al. [2025], Anthropic [2024], PassAgent provides: (1) `file_editor` for multi-file workspace manipulation, and (2) `pass_evaluator` for invoking the PassBench evaluation pipeline with three-stage diagnostics (pass matching → correctness → performance). The agent iteratively inspects target graphs, edits pass files, and refines based on *AS Score* feedback until convergence. All experiments in this paper are conducted on the fusible-subgraph tasks, using the ES_t formulation with $b = 0.1$ and $p = 0$. Full design details are in Appendix C.

Models and Baselines. We evaluate frontier models (GPT-5.4, Claude-Opus-4.6, Claude-Sonnet-4.6) and open-source models (GLM-5.1 GLM-5-Team et al. [2026], MiniMax-M2.7 MiniMaxAI [2026], Qwen3-30B-A3B and Qwen3-4B Qwen Team [2025]). Baselines include Eager execution and TorchInductor (`torch.compile`, default mode), preferred over `max-autotune` due to CUDA Graph layout freezing and overheads outweighing gains at this scale. Hardware details are in Appendix C.

4.2 Main Results

Table 1 presents results across five metrics (definitions in caption); we highlight four key findings.

(1) PassBench effectively discriminates model capabilities. The benchmark shows a clear performance gap: Claude-Sonnet-4.6 ($AS=0.448$) outperforms Qwen3-30B-A3B ($AS=0.139$) by $3.22\times$. Correctness ratios exhibit a similar spread (Sub. CR: 61.9% vs. 11.8%). This separation indicates that PassBench provides a meaningful discriminative signal across models.

(2) All models fall substantially short of the compiler baseline. All models have G-Mean Speedup below 1.0, meaning generated code is *slower* than eager execution. The best frontier model (Claude-Opus-4.6, G-Mean=0.922) approaches but does not reach parity, and the highest AS score (Claude-Sonnet-4.6, 0.448) trails Inductor (0.706) by 37%. Even for correct outputs, speedups rarely exceed $1.2\times$, indicating limited hardware-cost awareness in current LLM-generated kernels.

(3) Low aggregate scores coexist with striking individual successes. No model reaches $AS\geq 0.5$ or $G\text{-Mean}\geq 1.0$, yet on specific long-tail subgraphs, frontier models deliver up to $3.02\times$ speedup over Inductor (Section 4.4). The contrast between strong per-instance potential and weak aggregate performance reveals that the challenge is *consistency*: models fail to reliably generalize sparse successes across diverse patterns. Moreover, persistent failure modes including boundary misalignment, cost-model blindness, and semantic disruption suggest an unsaturated benchmark. Improving data and training infrastructure, rather than mere scaling, is key to closing this gap.

Model	fast_1(%) [*]	Samp. CR (%) [†]	Sub. CR (%) [‡]	G-Mean Speedup [§]	AS Score
Eager	100.0	100.0	100.0	1.000	1.000
Inductor	20.3	64.5	85.0	0.846	0.706
GPT-5.4	7.4	47.0	54.6	0.821	0.410
Claude-Opus-4.6	9.8	40.0	48.6	0.922	0.410
Claude-Sonnet-4.6	9.2	52.0	61.9	0.835	0.448
GLM-5.1	4.8	30.5	33.5	0.844	0.240
MiniMax-M2.7	1.0	23.5	23.0	0.653	0.208
Qwen3-4B	0.2	1.0	1.3	0.953	0.108
Qwen3-30B-A3B	0.6	7.5	11.8	0.693	0.139
Qwen3-4B-SFT [¶]	3.0	27.5	28.5	0.808	0.240
Qwen3-30B-A3B-SFT [#]	5.3	44.0	48.8	0.809	0.371

Table 1: **Main Results on PassBench.** ^{*}Fraction of correct subgraphs with speedup ≥ 1.0 over eager. [†]Fraction of correct samples. [‡]Fraction of correct subgraphs. [§]Geometric-mean speedup over correct subgraphs. [¶]Qwen3-4B fine-tuned on PassNet. [#]Qwen3-30B-A3B fine-tuned on PassNet.

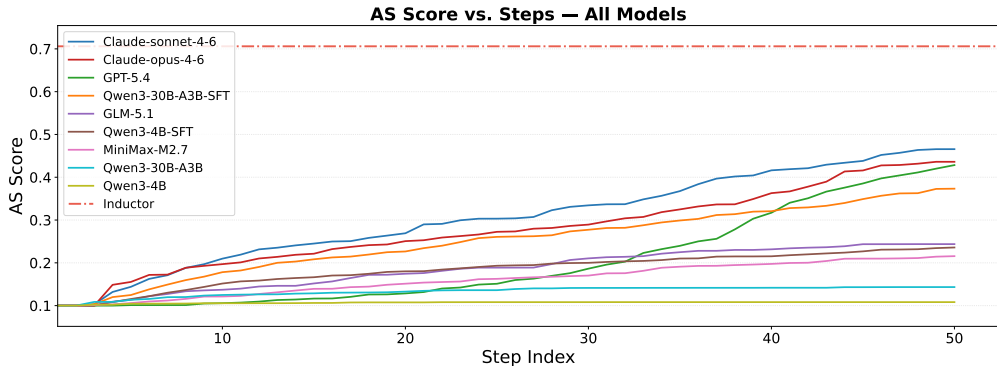


Figure 3: **Agent performance scales with iteration budget.** AS Score as a function of iteration steps (up to 50).

(4) Iteration reveals capabilities missed by single-shot evaluation. All main results are reported at convergence (50 iterations). As shown in Figure 3, a single evaluation captures only 31%–51% of each agent’s best AS score (mean 38%), and 12%–52% of eventually-passing samples exhibit non-monotonic *pass*→*fail*→*pass* trajectories as agents explore different generalization strategies. This differs from KernelBench, where iteration monotonically refines a single kernel.

4.3 Dataset Efficacy via Distillation

The main results show a large performance gap between frontier models and the open-source models. To address Q2, we distill expert trajectories into the smaller model and evaluate the resulting performance gains.

Setup. We generate PassAgent trajectories from 4, 476 samples using Claude-Sonnet-4.6 (two trials per instance, up to 50 iterations), retaining those with $AS > 0.1$ to obtain 3, 899 training trajectories. We then fine-tune Qwen3-30B-A3B and Qwen3-4B with learning rate 2×10^{-5} (cosine decay to 2×10^{-6}), batch size 8, 5 epochs, and 256K context length (full setup in Appendix C).

Results. Table 1 shows that “Qwen3-30B-A3B-SFT” yields an AS of 0.371, a $2.67 \times$ gain over the base model (0.139) and approaching frontier-model performance (0.410). Sub. CR and Samp. CR surge to 48.8% and 44.0% from 11.8% and 7.5%, respectively. Similar gains in Qwen3-4B-SFT, alongside scaling-driven improvements in the 30B variant, collectively validate our training dataset.

Table 2: **Sparkle Cases.** Speedups vs. Eager and Inductor on subgraphs where Inductor underperforms Eager.

Model (Pattern)	Dtype	vs. Eager	vs. Inductor	Max Diff	Kernels
MaskFormer (Roll+Slice)	bf16	1.65 ×	3.02 ×	0.031	6 → 1
BGE-Reranker (Masked Pool)	bf16	1.50 ×	2.90 ×	0.0	7 → 1

This result—achieved with only $\sim 4K$ trajectories from a single teacher—suggests substantial headroom through scaling data collection, multiple teachers, and RL from ES_t feedback.

4.4 Case Studies

We analyze representative successes and failures to understand the capabilities and limitations of current LLMs. Unlike kernel-centric approaches, pass generation enables LLMs to discover *graph-level rewrite rules*, i.e., pattern matchers paired with fused replacements that generalize across samples. Full implementations are provided in Appendix H.

Success Case 1: Roll+Slice Fusion (MaskFormer). TorchInductor decomposes `roll` into multiple `slice+cat` ops, launching 6 kernels for an 8-operator subgraph. The LLM recognizes the equivalence of `roll(shift=3) + slice[:128]` to index arithmetic ($\text{idx} = (S + i - \text{shift}) \bmod S$), replacing the entire subgraph with a single fused kernel (**3.02**× speedup).

Success Case 2: Masked Mean Pooling (BGE-Reranker). TorchInductor fails to fuse a 7-op chain (`cast→mul→sum→sum→clamp→div→cat`), yielding a $\sim 50\%$ slowdown vs. eager. The LLM identifies the masked mean pooling semantics and generates a single kernel that accumulates $\sum(\text{mask} \cdot \text{hidden})$ and $\sum(\text{mask})$ in FP32 registers (**2.90**× speedup, bitwise-identical).

In both cases, the compiler loses high-level semantics after decomposing operations into primitives; the LLM’s advantage is recognizing *composite intent* and directly lowering to fused implementations.

Failure Modes. Analysis identifies three systematic bottlenecks in agent-driven optimization: **(1) Boundary Misalignment**—Agents often misjudge arithmetic intensity, causing inefficient fusion of low-compute operators (e.g., ReLU) or redundant re-implementation of vendor-optimized primitives (e.g., Conv2d) in Triton. **(2) Cost-Model Blindness**—Lacking hardware awareness (e.g., register pressure, SRAM capacity), agents employ static tiling across varying shapes, resulting in significant gaps from roofline performance. **(3) Semantic Disruption**—Local rewrites frequently break optimization chains by replacing standard patterns with opaque kernels, disabling critical features like FlashAttention-2 routing. These issues indicate that PassBench poses open problems requiring hardware-aware reasoning beyond current LLM capabilities.

5 Conclusion and Future Work

We present **PassNet**, the first large-scale ecosystem for LLM-driven compiler pass generation, comprising: (1) **PassNet-Dataset**, featuring $18K$ unique computational graphs derived from 100K real-world models; and (2) **PassBench**, a suite of 200 curated long-tail tasks evaluated via the **Error-aware Speedup Score** (ES_t) with layered integrity defenses against LLM exploitation. Experiments demonstrate that PassBench is highly discriminative and unsaturated: while frontier models trail TorchInductor by 37% in aggregate, individual passes achieve up to $3\times$ speedup—identifying *consistency*, rather than capability, as the primary bottleneck. Notably, fine-tuning on $\sim 4K$ PassNet trajectories yields a $2.67\times$ performance gain, approaching frontier-model levels and validating PassNet as essential infrastructure for advancing LLM-driven compiler optimization.

Limitations and Future Directions. Current experiments focus on fusible tasks, following a curriculum that progresses from simpler cases to more challenging classical subgraph tasks. Accordingly, PassBench currently targets inference on a single GPU (NVIDIA A30), while generalization to training-loop optimizations, multi-device settings, and diverse hardware remains open. The dataset is skewed toward CV and NLP workloads (90.6% combined), which may limit coverage of emerging do-

mains such as scientific simulation and generative models. Our anti-cheating defenses, while effective against observed exploits, cannot guarantee completeness against future adversarial strategies.

Although evaluation graphs are sourced from public repositories, memorization risk is limited: pass generation requires producing executable pattern matchers and rewriters tailored to each graph structure, not reproducing code snippets; the multi-graph formulation further requires generalization across shapes and dtypes, reducing overfitting to specific instances.

Future directions include multi-device pass generation, extension to more complex tasks (e.g., classical subgraph tasks), integration of hardware cost models as auxiliary context, reinforcement learning from ES_t feedback, and continual expansion of the dataset to underrepresented domains. The entire ecosystem is publicly available.

References

- Tianqi Chen, Thierry Moreau, Ziheng Jiang, Lianmin Zheng, Eddie Yan, Meghan Cowan, Haichen Shen, Leyuan Wang, Yuwei Hu, Luis Ceze, Carlos Guestrin, and Arvind Krishnamurthy. Tvm: an automated end-to-end optimizing compiler for deep learning. In *USENIX Conference on Operating Systems Design and Implementation (OSDI)*, pages 579–594, 2018.
- Samuel J. Kaufman, Phitchaya Mangpo Phothilimthana, Yanqi Zhou, Charith Mendis, Sudip Roy, Amit Sabne, and Mike Burrows. A learned performance model for tensor processing units. In *Conference on Machine Learning and Systems (MLSys)*, 2021.
- Jason Ansel, Edward Yang, Horace He, Natalia Gimelshein, Animesh Jain, Michael Voznesensky, Bin Bao, Peter Bell, David Berard, Evgeni Burovski, et al. Pytorch 2: Faster machine learning through dynamic python bytecode transformation and graph compilation. In *International Conference on Architectural Support for Programming Languages and Operating Systems (ASPLOS)*, 2024.
- Anne Ouyang, Simon Guo, Simran Arora, Alex L Zhang, William Hu, Christopher Ré, and Azalia Mirhoseini. Kernelbench: Can llms write efficient gpu kernels? *arXiv preprint arXiv:2502.10517*, 2025.
- Weinan Dai, Hanlin Wu, Qiying Yu, Huan-ang Gao, Jiahao Li, Chengquan Jiang, Weiqiang Lou, Yufan Song, Hongli Yu, Jiaze Chen, et al. Cuda agent: Large-scale agentic rl for high-performance cuda kernel generation. *arXiv preprint arXiv:2602.24286*, 2026.
- Gang Liao, Hongsen Qin, Ying Wang, Alicia Golden, Michael Kuchnik, Yavuz Yetim, Jia Jiunn Ang, Chunli Fu, Yihan He, Samuel Hsia, et al. Kernelevolve: Scaling agentic kernel coding for heterogeneous ai accelerators at meta. *arXiv preprint arXiv:2512.23236*, 2025.
- Lianmin Zheng, Cheng Cheng, Eddie Yan, Haichen Ning, Cody Hao Yu, Thierry Moreau, Tianqi Chen, Carlos Guestrin, Arvind Krishnamurthy, and Luis Ceze. Anso: Generating high-performance tensor programs for deep learning. In *USENIX Symposium on Operating Systems Design and Implementation (OSDI)*, pages 935–950, 2020.
- Chris Leary and Todd Wang. Xla: Tensorflow, compiled. *TensorFlow Dev Summit*, 2(3), 2017.
- Junru Shao, Xiyu Zhou, Siyuan Feng, Bohan Hou, Ruihang Lai, Hongyi Jin, Wuwei Lin, Masahiro Masuda, Cody Hao Yu, and Tianqi Chen. Tensor program optimization with probabilistic programs. *Advances in Neural Information Processing Systems*, 35:35783–35796, 2022.
- Yaoyao Ding, Cody Hao Yu, Bojian Zheng, Yizhi Liu, Yida Wang, and Gennady Pekhimenko. Hidet: Task-mapping programming paradigm for deep learning tensor programs. In *ACM International Conference on Architectural Support for Programming Languages and Operating Systems (ASPLOS)*, pages 370–384, 2023.
- Zhen Zheng, Zaifeng Pan, Dalin Wang, Kai Zhu, Wenyi Zhao, Tianyou Guo, Xiafei Qiu, Minmin Sun, Junjie Bai, Feng Zhang, Xiaoyong Du, Jidong Zhai, and Wei Lin. Bladedisc: Optimizing dynamic shape machine learning workloads via compiler approach. *Proc. ACM Manag. Data*, pages 206:1–206:29, 2023a. URL <https://doi.org/10.1145/3617327>.
- Baidu PaddlePaddle Team. Cinn: Compiling intermediate representation to neural networks, 2021. URL <https://github.com/PaddlePaddle/CINN>. PaddlePaddle Compiler Infrastructure.
- Juyong Jiang, Fan Wang, Jiasi Shen, Sungju Kim, and Sunghun Kim. A survey on large language models for code generation. *ACM Transactions on Software Engineering and Methodology*, 2024.
- Zibin Zheng, Kaiwen Ning, Yanlin Wang, Jingwen Zhang, Dewu Zheng, Mingxi Ye, and Jiachi Chen. A survey of large language models for code: Evolution, benchmarking, and future trends. *arXiv preprint arXiv:2311.10372*, 2023b.
- Ke Liu, Qinglin Wang, Xiang Chen, Guang Yang, Yigui Feng, Gencheng Liu, and Jie Liu. Evaluating and improving framework-based parallel code completion with large language models. In *2025 40th IEEE/ACM International Conference on Automated Software Engineering (ASE)*, pages 2478–2490. IEEE, 2025.

- Kai Huang, Jian Zhang, Xiaofei Xie, and Chunyang Chen. Seeing is fixing: Cross-modal reasoning with multimodal llms for visual software issue repair. In *2025 40th IEEE/ACM International Conference on Automated Software Engineering (ASE)*, pages 1156–1168. IEEE, 2025.
- Boyang Yang, Haoye Tian, Jiadong Ren, Hongyu Zhang, Jacques Klein, Tegawendé F Bisseyandé, Claire Le Goues, and Shunfu Jin. Morepair: Teaching llms to repair code via multi-objective fine-tuning. *ACM Transactions on Software Engineering and Methodology*, 35(2):1–38, 2026.
- Carlos E. Jimenez, John Yang, Alexander Wettig, Shunyu Yao, Kexin Pei, Ofir Press, and Karthik Narasimhan. SWE-bench: Can language models resolve real-World GitHub issues? In *International Conference on Learning Representations (ICLR)*, 2024.
- John Yang, Carlos E. Jimenez, Alexander Wettig, Kilian Lieret, Shunyu Yao, Karthik Narasimhan, and Ofir Press. SWE-agent: Agent-computer interfaces enable automated software engineering. *arXiv preprint arXiv:2405.15793*, 2024.
- Xingyao Wang, Boxuan Chen, Yufan Yuan, Yuzhe Zhang, Bowen Li, Haotian Qian, Pengfei He, Ruiqi Lyu, Yikun Ma, Ziru Yu, et al. OpenHands: An open platform for AI software developers as generalist agents. *arXiv preprint arXiv:2407.16741*, 2024.
- Chris Cummins, Volker Seeker, Dejan Grubisic, Baptiste Roziere, Jonas Gehring, Gabriel Synnaeve, and Hugh Leather. Llm compiler: Foundation language models for compiler optimization. In *Proceedings of the 34th ACM SIGPLAN International Conference on Compiler Construction*, pages 141–153, 2025.
- Haolin Pan, Hongyu Lin, Haoran Luo, Yang Liu, Kaichun Yao, Libo Zhang, Mingjie Xing, and Yanjun Wu. Compiler-r1: Towards agentic compiler auto-tuning with reinforcement learning. *arXiv preprint arXiv:2506.15701*, 2025.
- Tianming Cui, Pen-Chung Yew, Stephen McCamant, and Antonia Zhai. Decos: Data-efficient reinforcement learning for compiler optimization selection ignited by llm. In *Proceedings of the 39th ACM International Conference on Supercomputing*, pages 943–958, 2025.
- Yi Zhai, Yu Zhang, Shuo Liu, Xiaomeng Chu, Jie Peng, Jianmin Ji, and Yanyong Zhang. Tlp: A deep learning-based cost model for tensor program tuning. In *Proceedings of the 28th ACM International Conference on Architectural Support for Programming Languages and Operating Systems, Volume 2*, pages 833–845, 2023.
- Yi Zhai, Sijia Yang, Keyu Pan, Renwei Zhang, Shuo Liu, Chao Liu, Zichun Ye, Jianmin Ji, Jie Zhao, Yu Zhang, et al. Enabling tensor language model to assist in generating high-performance tensor programs for deep learning. In *18th USENIX Symposium on Operating Systems Design and Implementation (OSDI 24)*, pages 289–305, 2024.
- Juncheng Dong, Yang Yang, Tao Liu, Yang Wang, Feng Qi, Vahid Tarokh, Kaushik Rangadurai, and Shuang Yang. Stark: Strategic team of agents for refining kernels. *arXiv preprint arXiv:2510.16996*, 2025.
- Carlo Baronio, Pietro Marsella, Ben Pan, Simon Guo, and Silas Alberti. Kevin: Multi-turn rl for generating cuda kernels. *arXiv preprint arXiv:2507.11948*, 2025.
- Jianghui Wang, Vinay Joshi, Saptarshi Majumder, Xu Chao, Bin Ding, Ziqiong Liu, Pratik Prabhanjan Brahma, Dong Li, Zicheng Liu, and Emad Barsoum. Geak: Introducing triton kernel ai agent & evaluation benchmarks, 2025. URL <https://arxiv.org/abs/2507.23194>.
- Qirui Zhou, Yuanbo Wen, Ruizhi Chen, Ke Gao, Weiqiang Xiong, Ling Li, Qi Guo, Yanjun Wu, and Yunji Chen. Qimeng-gemm: Automatically generating high-performance matrix multiplication code by exploiting large language models. In *Proceedings of the AAAI Conference on Artificial Intelligence*, volume 39, pages 22982–22990, 2025.
- Xiaoya Li, Xiaofei Sun, Albert Wang, Jiwei Li, and Chris Shum. Cuda-ll: Improving cuda optimization via contrastive reinforcement learning. *arXiv preprint arXiv:2507.14111*, 2025.
- Charles Hong, Sahil Bhatia, Alvin Cheung, and Yakun Sophia Shao. Autocomp: Llm-driven code optimization for tensor accelerators, 2025. URL <https://arxiv.org/abs/2505.18574>.

- Sharan Narang and Baidu Research. Deepbench: Benchmarking deep learning operations on different hardware, 2016. URL <https://github.com/baidu-research/DeepBench>.
- Peter Mattson, Vijay Janapa Reddi, Christine Cheng, Cody Coleman, Greg Diamos, David Kanter, Paulius Micikevicius, David Patterson, Guenther Schmuelling, Hanlin Tang, et al. Mlperf: An industry standard benchmark suite for machine learning performance. *IEEE Micro*, 40(2):8–16, 2020.
- Chris Cummins, Bram Wasti, Jiadong Guo, Brandon Cui, Jason Ansel, Sahir Gomez, Somya Jain, Jia Liu, Olivier Teytaud, Benoit Steiner, Yuandong Tian, and Hugh Leather. Compilergym: robust, performant compiler optimization environments for ai research. In *Proceedings of the 20th IEEE/ACM International Symposium on Code Generation and Optimization, CGO '22*, pages 92–105. IEEE Press, 2022. ISBN 9781665405843. doi: 10.1109/CGO53902.2022.9741258. URL <https://doi.org/10.1109/CGO53902.2022.9741258>.
- Aiden Grossman, Ludger Paehler, Konstantinos Parasyris, Tal Ben-Nun, Jacob Hegna, William S. Moses, Jose M Monsalve Diaz, Mircea Trofin, and Johannes Doerfert. Compile: A large IR dataset from production sources. *Journal of Data-centric Machine Learning Research*, 2024.
- Phitchaya Mangpo Phothilimthana, Sami Abu-El-Haija, Kaidi Cao, Bahare Fatemi, Michael Burrows, Charith Mendis, and Bryan Perozzi. Tpu graphs: A performance prediction dataset on large tensor computational graphs. In *Conference on Neural Information Processing Systems (NeurIPS)*, 2023.
- Lianmin Zheng, Ruochen Liu, Junru Shao, Tianqi Chen, Joseph E. Gonzalez, Ion Stoica, and Ameer Haj Ali. Tenset: A large-scale program performance dataset for learned tensor compilers. In *Conference on Neural Information Processing Systems ((NeurIPS))*, 2021.
- Chris Lattner, Mehdi Amini, Uday Bondhugula, Albert Cohen, Andy Davis, Jacques Pienaar, River Riddle, Tatiana Shpeisman, Nicolas Vasilache, and Oleksandr Zinenko. Mlir: Scaling compiler infrastructure for domain specific computation. In *International Symposium on Code Generation and Optimization (CGO)*, pages 2–14, 2021.
- Mingzhen Li, Yi Liu, Xiaoyan Liu, Qingxiao Sun, Xin You, Hailong Yang, Zhongzhi Luan, Lin Gan, Guangwen Yang, and Depei Qian. The deep learning compiler: A comprehensive survey. *IEEE Transactions on Parallel and Distributed Systems*, 32(3):708–727, 2021. ISSN 2161-9883. doi: 10.1109/tpds.2020.3030548.
- Naman Jain, Jaskirat Singh, Manish Shetty, Liang Zheng, Koushik Sen, and Ion Stoica. R2e-gym: Procedural environments and hybrid verifiers for scaling open-weights swe agents. *arXiv preprint arXiv:2504.07164*, 2025.
- Anthropic. Solving SWE-bench sonnet with Sonnet 3.5 and Anthropic agent infrastructure. <https://www.anthropic.com/engineering/swe-bench-sonnet>, 2024.
- GLM-5-Team, :, Aohan Zeng, Xin Lv, Zhenyu Hou, Zhengxiao Du, Qinkai Zheng, Bin Chen, Da Yin, Chendi Ge, Chenghua Huang, Chengxing Xie, Chenzheng Zhu, Congfeng Yin, Cunxiang Wang, Gengzheng Pan, Hao Zeng, Haoke Zhang, Haoran Wang, Huilong Chen, Jiajie Zhang, Jian Jiao, Jiaqi Guo, Jingsen Wang, Jingzhao Du, Jinzhu Wu, Kedong Wang, Lei Li, Lin Fan, Lucen Zhong, Mingdao Liu, Mingming Zhao, Pengfan Du, Qian Dong, Rui Lu, Shuang-Li, Shulin Cao, Song Liu, Ting Jiang, Xiaodong Chen, Xiaohan Zhang, Xuancheng Huang, Xuezhen Dong, Yabo Xu, Yao Wei, Yifan An, Yilin Niu, Yitong Zhu, Yuanhao Wen, Yukuo Cen, Yushi Bai, Zhongpei Qiao, Zihan Wang, Zikang Wang, Zilin Zhu, Ziqiang Liu, Zixuan Li, Bojie Wang, Bosi Wen, Can Huang, Changpeng Cai, Chao Yu, Chen Li, Chengwei Hu, Chenhui Zhang, Dan Zhang, Daoyan Lin, Dayong Yang, Di Wang, Ding Ai, Erle Zhu, Fangzhou Yi, Feiyu Chen, Guohong Wen, Hailong Sun, Haisha Zhao, Haiyi Hu, Hanchen Zhang, Hanrui Liu, Hanyu Zhang, Hao Peng, Hao Tai, Haobo Zhang, He Liu, Hongwei Wang, Hongxi Yan, Hongyu Ge, Huan Liu, Huanpeng Chu, Jia’ni Zhao, Jiachen Wang, Jiajing Zhao, Jiamin Ren, Jiapeng Wang, Jiabin Zhang, Jiayi Gui, Jiayue Zhao, Jijie Li, Jing An, Jing Li, Jingwei Yuan, Jinhua Du, Jinxin Liu, Junkai Zhi, Junwen Duan, Kaiyue Zhou, Kangjian Wei, Ke Wang, Keyun Luo, Laiqiang Zhang, Leigang Sha, Liang Xu, Lindong Wu, Lintao Ding, Lu Chen, Minghao Li, Nianyi Lin, Pan Ta, Qiang Zou, Rongjun Song, Ruiqi Yang, Shangqing Tu, Shangtong Yang, Shaoxiang Wu, Shengyan Zhang, Shijie Li, Shuang Li, Shuyi Fan, Wei Qin, Wei Tian, Weining Zhang, Wenbo Yu, Wenjie Liang, Xiang Kuang,

Xiangmeng Cheng, Xiangyang Li, Xiaoquan Yan, Xiaowei Hu, Xiaoying Ling, Xing Fan, Xingye Xia, Xinyuan Zhang, Xinze Zhang, Xirui Pan, Xu Zou, Xunkai Zhang, Yadi Liu, Yandong Wu, Yanfu Li, Yidong Wang, Yifan Zhu, Yijun Tan, Yilin Zhou, Yiming Pan, Ying Zhang, Yinpei Su, Yipeng Geng, Yong Yan, Yonglin Tan, Yuean Bi, Yuhan Shen, Yuhao Yang, Yujiang Li, Yunan Liu, Yunqing Wang, Yuntao Li, Yurong Wu, Yutao Zhang, Yuxi Duan, Yuxuan Zhang, Zezhen Liu, Zhengtao Jiang, Zhenhe Yan, Zheyu Zhang, Zhixiang Wei, Zhuo Chen, Zhuoer Feng, Zijun Yao, Ziwei Chai, Ziyuan Wang, Zuzhou Zhang, Bin Xu, Minlie Huang, Hongning Wang, Juanzi Li, Yuxiao Dong, and Jie Tang. Glm-5: from vibe coding to agentic engineering, 2026. URL <https://arxiv.org/abs/2602.15763>.

MiniMaxAI, 2026. URL <https://github.com/MiniMax-AI/MiniMax-M2.7>.

Qwen Team. Qwen3 technical report, 2025. URL <https://arxiv.org/abs/2505.09388>.

A Dataset Quality Constraints

A user’s model, wrapped by the `pass_net.extract`, is symbolically traced to generate a standardized set of files. This set forms a complete PassNet graph, including the high-level IR of the computation graph (`model.py`), metadata for inputs and weights (`input_meta.py`, `weight_meta.py`), SHA-based graph hash for deduplication (`graph_hash.txt`), and other components such as optional custom operator code.

We define five constraints applied to every computational graph in PassNet to ensure dataset quality and cross-platform compatibility:

- **Runnable:** Each graph must execute forward propagation under the designated framework without syntax errors or crashes.
- **Serializable:** Each sample and metadata must be serializable into standard formats (e.g., JSON) and correctly de-serializable.
- **Decomposable:** The entire computational graph must be decomposable into multiple non-overlapping subgraphs, where each subgraph represents an independent optimization unit. This supports compiler backends in performing fusion, scheduling, and other optimization tasks.
- **Statically Analyzable:** Operator names, types, and dependencies must be statically extractable (e.g., via `torch.fx`) for structural traversal. This allows automated analysis tools to fully interpret operator semantics for structural traversal and pattern matching.
- **Custom Operator Accessible:** If a sample includes user-defined custom operators, the corresponding source code for these operators must be traceable and accessible in a modular form, ensuring reusability and integration across compiler environments.

B PassBench Sampling Details

Multi-dimensional Bucketing. Subgraphs are grouped into discrete buckets defined by three complementary dimensions:

- **Operator Sequence:** The ordered operator-name list serves as an exact-match key.
- **Input Shape:** We apply logarithmic quantization $\lfloor \log_2(d)/4 \rfloor$ to each dimension d , where the scaling factor 4 is empirically chosen to balance granularity and generalization.
- **Input Dtype:** Exact-match key for numerical precision.

Hierarchical Representative Grouping. Following bucketing, we employ a hierarchical strategy to select representative subgraphs and construct groups with varying cardinalities, each corresponding to a PassBench sample. The group size controls the optimization difficulty, as larger and more heterogeneous groups require transformations that generalize across a broader set of subgraphs.

- **Intra-bucket Stratified Sampling:** Within each operator sequence, subgraphs are sampled at a fixed stride σ , and then organized into groups of size 1 and 3, capturing both single-operator cases and short compositional patterns.
- **Cross-shape Structural Aggregation:** For each unique operator sequence, one representative is aggregated with subgraphs sharing the same sequence across different input shape buckets.
- **Precision-aware Coverage:** Within each shape bucket, subgraphs with distinct data types (FP32, FP16, BF16) are aggregated to ensure numerical format coverage.

C Experimental Setup

C.1 Benchmark Evaluation

Table 3 summarizes the hardware and evaluation protocol used across all PassBench experiments.

C.2 Distillation and Post-training

Table 4 details the teacher-student configuration and SFT hyperparameters.

Category	Detail
GPU	NVIDIA A30, 24 GB, compute capability 8.0
CUDA / cuDNN	12.8 / 9.10.2
PyTorch / Triton	2.9.1+cu128 / 3.5.1
Operating System	Ubuntu 24.04.1 LTS
Evaluation Mode	Single-shot, temperature= 0
Warmup Runs	20
Timed Trials	100
Stability Criterion	Re-run if IQR > 20% of median

Table 3: **Evaluation environment and benchmark protocol.**

Category	Detail
Teacher Agent	Claude-Sonnet-4.6
Max Trajectory Steps	50 per instance
Filtering Criterion	AS score > 0.1
Instances Processed	4,476 (2 trials each)
Trajectories Retained	3,899
Student Model	Qwen3-30B-A3B-Thinking-2507
Initial Learning Rate	2×10^{-5} (cosine decay to 2×10^{-6})
Batch Size	8
Epochs	5
Max Context Length	262,144

Table 4: **Distillation and post-training configuration.**

D Graph-level Interpretation of ES_t

In this section, we show that ES_t can be equivalently expressed as a geometric mean of per-graph error-aware rectified speedups.

We first define $r_{t,i}$, the penalty factor for erroneous graphs that captures tolerance-dependent penalties. The per-graph error-aware rectified speedup $\hat{s}_{t,i}$ (defined in Section 3.5) uses $r_{t,i}$ in its third case.

Definition D.1 (Penalty Factor). For each erroneous graph i , let $c_i \in \{1, 2, 3\}$ denote its error category. Let N_{err} be the number of erroneous graphs, and N_c be the number of graphs with error category c . The *penalty factor* is

$$r_{t,i} = \begin{cases} b, & t < c_i, \\ 1, & \text{otherwise,} \end{cases} \quad (5)$$

where $b \in (0, 1)$ is the base penalty.

Let $\pi_c = N_c/N_{\text{err}}$ denote the fraction of error category c among all erroneous graphs.

Definition D.2 (Error-aware Speedup Score ES_t). The macro-level Error-aware Speedup Score ES_t admits the following factored form:

$$ES_t = \alpha^\lambda \cdot \beta^{\lambda\eta(p+1)} \cdot \gamma_t^{1-\lambda} \quad (6)$$

where $\gamma_t = b^{\sum_{c \in \{1,2,3\}} \pi_c \mathbf{1}(t < c)}$. Here α aggregates correct-and-fast subgraphs, β penalizes correct-but-slow ones, and γ_t accounts for errors under tolerance t .

Proposition D.1 (Geometric mean of penalty factors). *The aggregated penalty γ_t equals the geometric mean of $\{r_{t,i}\}$ over all erroneous graphs:*

$$\gamma_t = \left(\prod_{i=1}^{N_{\text{err}}} r_{t,i} \right)^{1/N_{\text{err}}} \quad (7)$$

From the definition of $r_{t,i}$, each term contributes b iff $t < c_i$:

$$\prod_{i=1}^{N_{\text{err}}} r_{t,i} = \prod_{i=1}^{N_{\text{err}}} b^{\mathbf{1}(t < c_i)} = b^{\sum_{i=1}^{N_{\text{err}}} \mathbf{1}(t < c_i)}$$

Grouping by error category c gives

$$\sum_{i=1}^{N_{err}} \mathbf{1}(t < c_i) = \sum_{c \in \{1,2,3\}} N_c \mathbf{1}(t < c)$$

thus

$$\prod_{i=1}^{N_{err}} r_{t,i} = b^{\sum_{c \in \{1,2,3\}} N_c \mathbf{1}(t < c)}$$

Taking the N_{err} th root:

$$\left(\prod_{i=1}^{N_{err}} r_{t,i} \right)^{1/N_{err}} = b^{\frac{1}{N_{err}} \sum_{c \in \{1,2,3\}} N_c \mathbf{1}(t < c)} = b^{\sum_{c \in \{1,2,3\}} \pi_c \mathbf{1}(t < c)}$$

which is exactly the definition of γ_t .

Proposition D.2 (Geometric mean of per-graph speedups). *Since γ_t is the geometric mean of $\{r_{t,i}\}$ for a given t , the macro-level metric ES_t equals the geometric mean of per-graph error-aware rectified speedups:*

$$ES_t = \left(\prod_{i=1}^N \hat{s}_{t,i} \right)^{1/N} \quad (8)$$

This follows from the factored form: α , β , and γ_t are respectively the geometric means of the speedups from the correct-fast, correct-slow, and erroneous cases in $\hat{s}_{t,i}$. Their product therefore equals the geometric mean of all $\{\hat{s}_{t,i}\}$.

E Aggregated Speedup (AS) Weight Specification

The Aggregated Speedup aggregates the tolerance-parameterized ES_t into a single scalar via a normalized geometric mean (Section 3.5). Given the weight function W_t , AS is defined as:

$$AS = \prod_{t=-10}^{|E|+1} ES_t^{W_t / \sum_{s=-10}^{|E|+1} W_s} \quad (9)$$

The weight function W_t is defined as:

$$W_t = \begin{cases} 0.001 & \text{if } -10 \leq t \leq -6 \text{ or } t \geq |E| + 1, \\ 1 & \text{if } -5 \leq t \leq -3, \\ 0.8^{t+3} & \text{if } -2 \leq t \leq |E|. \end{cases} \quad (10)$$

Design Rationale. The weight schedule reflects three regimes:

- **Strict-correctness regime** ($t \in [-5, -3]$, $W_t = 1$): Production-level accuracy; full weight.
- **Relaxed regime** ($t \in [-2, |E|]$, $W_t = 0.8^{t+3}$): Exponential decay as correctness becomes easier to satisfy.
- **Extreme regime** ($t \leq -6$ or $t \geq |E| + 1$, $W_t = 0.001$): Near-zero weight to avoid distortion from ultra-strict or ultra-relaxed tolerances.

F Configuration of atol(t) and rtol(t)

We perform log-linear interpolation between reference points (e.g., $\text{atol}_{\text{fp32}}(-5) = 10^{-5}$ and $\text{atol}_{\text{fp32}}(0) = 1$) such that $\text{atol}(t), \text{rtol}(t) = 10^{kt}$.

G TorchInductor Default Pipeline Profiling

To empirically quantify the long-tail optimization gap discussed in Section 1, we profile TorchInductor’s default pass pipeline (`torch.compile(mode="default")`) on a large-scale subgraph corpus.

Data Type	atol(t)	atol(-5)	atol(0)
bfloat16	10^t	1e-5	1
float16/complex32	10^t	1e-5	1
float32/complex64	10^t	1e-5	1
float64/complex128	$10^{t-7/5}$	1e-7	1
others	0.0	0.0	0.0

Table 5: atol configuration (abbreviated)

Data Type	rtol(t)	rtol(-5)	rtol(0)
bfloat16	$10^{t-1.796/5}$	1.6e-2	1
float16/complex32	$10^{t-3/5}$	1e-3	1
float32/complex64	$10^{t-5.886/5}$	1.3e-6	1
float64/complex128	$10^{t-7/5}$	1e-7	1
others	0.0	0.0	0.0

Table 6: rtol configuration (abbreviated)

Setup. We extract 9,526 subgraphs from 1,000 community models via `torch.fx` graph tracing: 56.9% from HuggingFace Transformers (BERT, T5, LLaVA, Qwen-VL, etc.) and 43.1% from timm (ResNet, EfficientNet, ViT, FastViT, etc.). Subgraph node counts range from 4 to 63 (median 16). Experiments run on NVIDIA A30 GPUs (24 GiB) with PyTorch 2.9.1 and CUDA 12.8. Each subgraph is benchmarked with 20 warmup iterations and 100 timed trials; we report median latencies and reject samples with unstable timing (IQR/median > 20%).

Compilation Success. Of the 9,526 subgraphs, 84.5% compile successfully and pass correctness verification. The majority of failures (72.8%) stem from GPU timing instability in the shared cloud environment (IQR/median exceeding our 20% stability threshold); these samples are excluded as invalid measurements. The compiler-specific failure rate is 3.1%, concentrated on non-standard architectures (LeViT, GCViT) with unconventional reshape and attention-head operations.

Kernel Speedup Distribution. Table 7 reports the kernel-level speedup distribution over the 8,021 subgraphs with valid performance data.

Speedup Range	Fraction
< 1.0× (degradation)	8.3%
1.0–1.2× (marginal)	26.6%
1.2–2.0×	37.4%
≥ 2.0×	27.2%

Table 7: **Kernel speedup distribution under TorchInductor’s default pipeline.** Over one-third of subgraphs receive less than 1.2× kernel acceleration.

End-to-End Slowdown Analysis. Of the 43% of subgraphs that exhibit E2E slowdowns, the majority are *not* caused by kernel-level regression. Table 8 decomposes the 3,479 E2E bad cases by root cause.

Root Cause	Fraction	Median E2E Speedup
Small-graph fixed overhead (< 15 nodes)	61.5%	0.68×
Fast-model dispatch overhead (≥ 15 nodes, eager < 2 ms)	18.7%	0.89×
True kernel degradation	18.3%	0.86×
Other (marginal)	1.5%	0.99×

Table 8: **Root-cause decomposition of E2E slowdowns.** In 80.2% of cases, kernels are actually faster (median 1.21×), but a fixed dispatch overhead of ~0.14 ms from `torch.compile` negates the gain.

Subgraph size is the primary determinant: the E2E bad rate drops from 85.8% for subgraphs with 1–5 nodes to 13.0% for those with 30–50 nodes (median subgraph size: 9 nodes for bad cases vs. 29 for good cases). This confirms that the E2E overhead is largely a framework infrastructure cost orthogonal to pass-level optimization quality. True kernel degradation accounts for only 18.3% of E2E bad cases and is concentrated on FastViT-family architectures with non-standard attention mechanisms.

Numerical Precision. Among the 8,027 correctly compiled subgraphs, 39.7% produce bitwise-identical outputs and 81.5% exhibit maximum absolute difference below 10^{-6} . A small fraction

(4.6%) shows deviations $\geq 10^{-3}$, typically correlated with aggressive fusion strategies that yield higher speedups (mean kernel speedup $3.03\times$ vs. $2.09\times$ for precise cases).

ES(t) Scores. Evaluating TorchInductor under our ES_t metric yields a G-Mean Speedup of 0.846 and an AS Score of 0.706 (Table 1), confirming substantial room for improvement when correctness and stability are jointly considered.

H Detailed Sparkle Case Analysis

This appendix provides the complete pass files for the sparkle cases discussed in Section 4.

H.1 Case 1: Index-Arithmetic Roll+Slice Fusion (MaskFormer)

The MaskFormer pass targets an 8-operator subgraph in MaskFormer’s pixel decoder. Its operator sequence is `contiguous→view→roll→slice→contiguous→view→add→layer_norm`; under default compilation, this launches 6 separate kernels. The LLM recognizes that `roll(shift=3)+slice[:128]` on a $[S, S, C]$ tensor can be replaced by direct index arithmetic `input_i = (S + i - shift) mod S`, and additionally fuses the layer-norm reduction via shared-memory accumulation. Crucially, the replacement produces **two outputs** (add result and layer-norm result) in a single kernel.

The pass is split into a **shared lowering module** and a **shape-specific pattern pass**. The shared module contains the CUDA kernel, the inline loader registration, and a routing dispatch that parameterizes the kernel for three Swin-Transformer stages (D=96, 192, 384). All shape-specific passes import the same shared module and differ only in their `pattern` and `replacement_args`, demonstrating the reusability of a single lowering across multiple FX pattern instances.

Shared lowering module (`shared_fused_roll_add_ln.py` with inline CUDA):

```
import torch
from torch.utils.cpp_extension import load_inline

_cuda_src = r"""
#include <torch/extension.h>
#include <cuda_runtime.h>

template<typename scalar_t>
__global__ void fused_roll_slice_add_layernorm_kernel(
    const scalar_t* __restrict__ input_6d,
    const scalar_t* __restrict__ residual,
    const scalar_t* __restrict__ weight,
    const scalar_t* __restrict__ bias,
    scalar_t* __restrict__ out_add,
    scalar_t* __restrict__ out_ln,
    const int R, const int C, const int S, const int SC, const int shift
) {
    const int row = blockIdx.x;
    if (row >= R) return;

    extern __shared__ float smem[];
    const int tid = threadIdx.x;

    // Index arithmetic: roll(shift,dims=[0,1]) on [S,S,C] then slice [:SC,:SC,:]
    const int i = row / SC;
    const int j = row % SC;
    const int input_i = (S + i - shift) % S;
    const int input_j = (S + j - shift) % S;

    // Pass 1: accumulate mean of (residual + rolled_input) via shared memory
    float local_sum = 0.0f;
```

```

for (int col = tid; col < C; col += blockDim.x) {
    float rolled = static_cast<float>(
        input_6d[input_i * S * C + input_j * C + col]);
    float res = static_cast<float>(residual[row * C + col]);
    local_sum += res + rolled;
}
smem[tid] = local_sum;
// shared-memory reduction to mean ...
const float mean = smem[0] / static_cast<float>(C);

// Pass 2: accumulate variance
float local_var = 0.0f;
for (int col = tid; col < C; col += blockDim.x) {
    float rolled = static_cast<float>(
        input_6d[input_i * S * C + input_j * C + col]);
    float res = static_cast<float>(residual[row * C + col]);
    float diff = (res + rolled) - mean;
    local_var += diff * diff;
}
smem[tid] = local_var;
// shared-memory reduction to variance ...
const float inv_std = rsqrtf(smem[0] / static_cast<float>(C) + 1e-5f);

// Pass 3: write both outputs
for (int col = tid; col < C; col += blockDim.x) {
    float rolled = static_cast<float>(
        input_6d[input_i * S * C + input_j * C + col]);
    float res = static_cast<float>(residual[row * C + col]);
    float added = res + rolled;
    out_add[row * C + col] = static_cast<scalar_t>(added);
    float normed = (added - mean) * inv_std;
    out_ln[row * C + col] = static_cast<scalar_t>(
        normed * static_cast<float>(weight[col])
        + static_cast<float>(bias[col]));
}
}
// Host wrapper omitted for brevity; allocates out_add/out_ln,
// chooses threads via next-power-of-two heuristics, and launches.
"""

_ext = load_inline(
    name="fused_roll_slice_add_layernorm_ext",
    cuda_sources=_cuda_src,
    functions=["fused_roll_slice_add_layernorm_cuda"],
    verbose=False,
)

@torch.fx.wrap
def fused_roll_slice_add_layernorm_dispatch(in_3, in_2, in_1, in_0, route):
    if route == "D96":
        return _ext.fused_roll_slice_add_layernorm_cuda(
            in_3, in_2, in_1, in_0, 133, 128, 3, 1e-5)
    elif route == "D192":
        return _ext.fused_roll_slice_add_layernorm_cuda(
            in_3, in_2, in_1, in_0, 70, 64, 3, 1e-5)
    elif route == "D384":
        return _ext.fused_roll_slice_add_layernorm_cuda(
            in_3, in_2, in_1, in_0, 35, 32, 3, 1e-5)

```

```

else:
    raise ValueError(f"Unknown route: {route}")

```

Shape-specific pattern pass (FusedRollSliceAddLayerNorm_96.py, D=96 stage):

```

import torch
from pass_dir.shared_fused_roll_add_ln import fused_roll_slice_add_layernorm_dispatch

```

```

def pattern(in_0, in_1, in_2, in_3):
    tmp_2 = in_3.contiguous()
    tmp_3 = tmp_2.view(-1, 133, 133, 96)
    tmp_4 = torch.roll(tmp_3, shifts=(3, 3), dims=(1, 2))
    tmp_5 = tmp_4[(slice(None, None, None), slice(None, 128, None),
                  slice(None, 128, None), slice(None, None, None))]
    tmp_6 = tmp_5.contiguous()
    tmp_7 = tmp_6.view(1, 16384, 96)
    tmp_8 = in_2 + tmp_7
    tmp_9 = torch.nn.functional.layer_norm(tmp_8, (96,), in_1, in_0, 1e-05)
    return (tmp_8, tmp_9)

```

```

def replacement_args(in_0, in_1, in_2, in_3):
    return (in_3, in_2, in_1, in_0, "D96")

```

```

def replacement_func():
    return fused_roll_slice_add_layernorm_dispatch

```

H.2 Case 2: Pattern-Driven Masked Mean Pooling (BGE-Reranker)

The BGE-Reranker pass targets a 7-operator subgraph in the sentence-embedding module. Its operator sequence is `cast→mul→sum→sum→clamp→div→cat`; under default compilation, this launches 7 separate kernels because the compiler treats the two reductions independently. The LLM recognizes the semantic intent as “masked mean pooling” and generates a rewrite that fuses all operators into a single kernel, accumulating $\sum(\text{mask} \cdot \text{hidden})$ and $\sum(\text{mask})$ simultaneously in float32 registers.

Shared lowering module (shared_cuda_bge.py with inline CUDA):

```

import torch
from torch.utils.cpp_extension import load_inline

_cuda_src = r"""
#include <torch/extension.h>
#include <cuda_runtime.h>

template<typename hidden_t>
__global__ void masked_mean_pooling_kernel(
    const float* __restrict__ mask,
    const hidden_t* __restrict__ hidden,
    float* __restrict__ output,
    const int S, const int D
) {
    const int bid = blockIdx.x;
    const int d_idx = blockIdx.y * blockDim.x + threadIdx.x;
    if (d_idx >= D) return;

    const float* mask_batch = mask + bid * S * D;
    const hidden_t* hidden_batch = hidden + bid * S * D;

```

```

float acc_val = 0.0f;
float acc_mask = 0.0f;
for (int s = 0; s < S; ++s) {
    int offset = s * D + d_idx;
    acc_val += static_cast<float>(hidden_batch[offset]) * mask_batch[offset];
    acc_mask += mask_batch[offset];
}
output[bid * D + d_idx] = acc_val / (acc_mask > 1e-9f ? acc_mask : 1e-9f);
}
// Host wrapper omitted for brevity; converts mask to float32,
// allocates [B,D] float32 output, and launches with dim3(B, ceil(D/128)).
"""

```

```

_ext = load_inline(
    name="fused_masked_mean_pooling_cuda_ext",
    cuda_sources=_cuda_src,
    functions=["fused_masked_mean_pooling_cuda"],
    verbose=False,
)

```

```

@torch.fx.wrap
def fused_masked_mean_pooling(in_0, in_1):
    return _ext.fused_masked_mean_pooling_cuda(in_0, in_1)

```

Pattern pass (FuseMaskedMeanPooling.py):

```

import torch
from pass_dir.shared_cuda_bge import fused_masked_mean_pooling

```

```

def pattern(in_0, in_1):
    tmp_0 = in_0.to(torch.float32)
    tmp_1 = in_1 * tmp_0
    tmp_2 = torch.sum(tmp_1, 1)
    tmp_3 = tmp_0.sum(1)
    tmp_4 = torch.clamp(tmp_3, min=1e-09)
    tmp_5 = tmp_2 / tmp_4
    tmp_6 = torch.cat([tmp_5], 1)
    return tmp_6

```

```

def replacement_args(in_0, in_1):
    return (in_0, in_1)

```

```

def replacement_func():
    return fused_masked_mean_pooling

```

Key implementation notes. The kernel performs two sequential reductions (`acc_val` and `acc_mask`) in float32 over the sequence dimension S , matching the eager-mode cast-to-float32 semantics. The output shape is $[B, D]$, where B is the batch size and D is the hidden dimension. Because the eager pattern includes a no-op `cat` (concatenating a single tensor along dim 1), the replacement preserves the original output shape without additional reshaping. The same rewrite rule applies to varying sequence lengths and hidden dimensions without recompilation.